This is a repository copy of *Is the S2N2 ring a singlet diradical? Critical analysis of alternative valence bond descriptions*.

# Spin-Coupled Generalized Valence Bond (SCGVB) Descriptions of $\pi$-Electron Systems in $S_2N_2$ and $S_4N_4^{2+}$ Rings

Fabio E. Penotti,[†] David Cooper,*,[‡] and Peter B. Karadakov[§]

[†]Consiglio Nazionale delle Ricerche, Istituto di Scienze e Tecnologie Molecolari, Via Golgi 19, I−20133 Milano MI, Italy

[‡]Department of Chemistry, University of Liverpool, Liverpool L69 7ZD, UK

[§]Department of Chemistry, University of York, Heslington, York YO10 5DD, UK

**ABSTRACT:** Rival spin-coupled generalized valence bond (SCGVB) solutions are investigated for the $\pi$-electron systems of the $S_2N_2$ and $S_4N_4^{2+}$ rings near equilibrium geometry. The preferred compact SCGVB description is provided in each case by the variational optimization of two configurations that turn out to be symmetry related to one another. Optimization instead of symmetry-pure single-configuration SCGVB wave functions leads to the involvement of three-center SNS or NSN orbitals, which seems to be an unnecessary complication. In neither case is very much achieved from the mixing of competing solutions. Breathing orbital VB (BOVB) calculations for $S_2N_2$ confirm a structure with NN singlet diradical character to be more important than one with SS singlet diradical character, but the largest contribution (*ca*. 60%) turns out to be due to the symmetry-determined linear combination of four symmetry-equivalent structures that lack any obvious diradical character. Much the same pattern was consistently found when we used a simple but robust projection of our various SCGVB wave functions for $S_2N_2$ onto the basis of BOVB structures (plus an orthogonal complement).

## 1. INTRODUCTION

Although various $(SN)_x$ systems continue to attract considerable experimental and theoretical attention for a wide range of reasons, we should admit from the outset that our own particular interest in the planar $S_2N_2$ ring is somewhat more prosaic. A spin-coupled generalized valence bond (SCGVB) description of $S_2N_2$, reported by Gerratt et al.,[1] was interpreted at the time as being dominated by SS singlet diradical character. Some other studies,[2,3,4,5] and especially the very careful breathing orbital valence bond (BOVB) work of Braïda et al.,[2] have seriously questioned the validity of that interpretation. Indeed, Braïda et al.[2] were able to show by partly qualitative arguments that the SCGVB wave function, when stripped to some extent of the delocalization tails on the fully-optimized active orbitals, did in fact appear to be consistent with the BOVB viewpoint, in which a structure with NN singlet diradical character was the largest single contributor. We re-examine this issue in the present work, using a robust projection of the SCGVB wave function onto the basis of the BOVB structures. While confirming the main gist of the conclusions of Braïda et al.,[2] namely that Gerratt et al.[1] may have misinterpreted the results of their SCGVB calculations, we also show that the interpretation of the BOVB description could be slightly more nuanced than had been supposed. Additionally, as was shown by Thorsteinsson et al.,[6] there can exist rival SCGVB-like solutions that are fairly close in energy to the one described by Gerratt et al..[1] We explore this issue further and then require different combinations of SCGVB solutions to fight it out without any prejudice in a variational boxing ring, thereby obtaining further insight into the bonding in the $\pi$-electron system of $S_2N_2$. We then examine briefly certain analogous rival SCGVB descriptions of the corresponding $\pi$-electron system in the $S_4N_4{}^{2+}$ ring.

## 2. THEORETICAL AND COMPUTATIONAL DETAILS

The single-configuration SCGVB wave function for the valence $\pi$-space of $S_2N_2$ is based on a single product of six singly-occupied nonorthogonal active orbitals $\pi_\mu$ that are expanded in the full basis set and it can be written in the following form:[7]

$$\Psi_{\text{SCGVB}} = \mathcal{A} \left[ \left( \prod_{i=1}^{18} \varphi_i \alpha \varphi_i \beta \right) \left( \prod_{\mu=1}^{6} \pi_\mu \right) \Theta_0^6 \right] \tag{1}$$

in which the $\varphi_i$ are doubly-occupied inactive orbitals that accommodate the 'core' $S(2p_\pi)$ electrons and all of the $\sigma$ system. The active-space total spin function $\Theta_0^6$ is expanded in the full spin space of five linearly-independent modes of coupling together the spins of six electrons so as to achieve an overall singlet state, with the expansion coefficients known as spin-coupling coefficients. Traditionally, wave functions of this type, as introduced by Gerratt,[8] have mostly been termed spin-

coupled (SC or even SCVB), with an acknowledgement that the construction is in fact entirely equivalent to that of *full* generalized valence bond (full-GVB), as introduced by Goddard,[9] or they have been called (full-)GVB, with a mention of the equivalence to SC (or SCVB). It seems to the present authors to be undesirable to persist with different names for essentially identical calculations that might even have been carried out with the same codes. Accordingly, we use here instead the compound term spin-coupled generalized valence bond (SCGVB) that aims to encompass both sets of names, and we recommend that others consider doing the same.

Following fairly closely the construction used by Braïda et al.,[2] our BOVB calculations for $S_2N_2$ were carried out using six VB structures (see Figure 1), with each of the symmetry-unique active $\pi$ orbitals in each structure optimized as an entirely separate linear combination of the basis functions centered on the relevant nucleus. Where there are two electrons associated with the same center, they are accommodated with opposing spins in the same orbital. As can be seen from Figure 1, BOVB structure **1** clearly corresponds to NN singlet diradical character and BOVB structure **2** to SS singlet diradical character. The four symmetry-equivalent BOVB structures **3** to **6** each feature instead one S−N $\pi$ bond. (We subsequently also carried out S-BOVB calculations in which each of the doubly occupied active orbitals was allowed to 'split' into two singly occupied orbitals, but maintaining singlet coupling for the two orbitals.)

«Figure 1 near here»

All of our electronic structure calculations for $S_2N_2$ were carried out for the nuclear geometry and orientation shown in Figure 2 and using the standard cc-pVQZ basis set. We have intentionally chosen the same idealized square geometry, close to experiment, that was used by Gerratt et al.,[1] but we are confident that all of our key findings will be relatively insensitive to small changes to this geometry. Instead of optimizing each time the various inactive orbitals in our various VB descriptions of $S_2N_2$, we have chosen to take those orbitals without any further reoptimization from an appropriate CASSCF description that should not introduce any significant bias for or against the various competing VB descriptions of the valence $\pi$ systems. Following various numerical tests of different choices of CASSCF inactive spaces (see Table S1 in the Supporting Information) we selected a six electrons in eight orbitals expansion spanning $3 \times B_{1u} + 2 \times B_{2g} + 2 \times B_{3g} + A_u$, which we abbreviate to [3,2,2,1]. Note that we were unable in our BOVB and S-BOVB calculations to orthogonalize the active $\pi$ orbitals to the two fixed 'core' $\pi$ MOs ($B_{1u} + B_{2g}$) taken from the CASSCF, because of the strict localization constraints on the active orbitals. In order to avoid numerical problems, we identified in the S atomic basis set the $2p_\pi$ contraction which contributes most to the inactive $\pi$ orbitals and then constrained to zero its coefficients in the expansions of the active orbitals. Such constraints

3

were not necessary in any of the SCGVB calculations for $S_2N_2$. We did, however, check that changes to SCGVB energies upon the application of such constraints are negligible.

Our subsequent SCGVB calculations for the valence $\pi$-space of the planar $S_4N_4^{2+}$ ring were carried out for the geometry and orientation shown in Figure 2 and again using the standard cc-pVQZ basis set. The SN nuclear separation, the bond angles and the molecular point group ($D_{4h}$) were based on the crystallographic studies of Gillespie et al.[10] but, as in the case of $S_2N_2$, we do not expect any of our key findings to be sensitive to small changes to this geometry. Our single-configuration SCGVB wave function for the valence $\pi$-space of $S_4N_4^{2+}$ is based on a single product of ten singly-occupied nonorthogonal active orbitals $\pi_\mu$ that are expanded in the full basis set and it can be written in the following form:[7]

$$\Psi_{\text{SCGVB}} = \mathcal{A}\left[\left(\prod_{i=1}^{40} \varphi_i \alpha \varphi_i \beta\right)\left(\prod_{\mu=1}^{10} \pi_\mu\right)\Theta_0^{10}\right] \tag{2}$$

in which the active-space total spin function $\Theta_0^{10}$ is expanded in the full spin space, consisting of 42 linearly-independent modes of coupling together the spins of ten electrons so as to achieve an overall singlet state. For all of our frozen-core VB calculations on $S_4N_4^{2+}$ we took the doubly-occupied inactive orbitals $\varphi_i$ that accommodate the 'core' $S(2p_\pi)$ electrons and all of the $\sigma$ system from a full-valence $\pi$-space CASSCF(10,8) wave function, without further optimization.

For a normalized wave function $\Psi$ that is expressed as a linear combination of nonorthogonal VB structures or configurations $\Phi_k$ with expansion coefficients $c_k$, it is most usual to assess the relative importance of the various $\Phi_k$ according to their Chirgwin-Coulson weights, $W_k$, which may be defined according to:[11]

$$W_k = c_k \sum_l c_l \langle \Phi_k | \Phi_l \rangle \tag{3}$$

in which the $W_k$ sum to unity, so as to satisfy the normalization condition for $\Psi$. This widely-used definition of weights has a number of useful properties except that, especially in the case of high values of the overlaps $S_{kl} = \langle \Phi_k | \Phi_l \rangle$, individual values of $W_k$ can occasionally fall outside the physically-meaningful range of 0 to 1. In addition to the Chirgwin-Coulson scheme, we also make some use in the present work of the inverse-overlap definition of Gallup and Norbeck:[12]

$$w_k = |c_k|^2 / (\boldsymbol{S}^{-1})_{kk} \tag{4}$$

where the values of $w_k$ are usually renormalized so as to add to unity. Such values then necessarily lie in the physically-meaningful range (0 to 1).

The workhorse for all of the VB calculations reported here was the generalized multiconfiguration spin-coupled (GMCSC) program developed by Penotti,[13] with CASSCF inactive

orbitals and the required integrals over basis functions generated using the GAMESS-US package.[14] Pictorial depictions of SCGVB active orbitals were produced using Virtual Reality Markup Language (VRML) files generated with Molden.[15] Quantum theory of atoms in molecules (QTAIM) analysis[16] was performed using AIMAll[17] and with our own codes. Additional $\pi$-space CASSCF calculations were carried out in $D_{2h}$ symmetry using MOLPRO.[18]

## 3. RESULTS AND DISCUSSION

**3.1. $S_2N_2$.** It is useful to consider first a single-configuration SCGVB wave function for $S_2N_2$ that is based on active orbitals which span the space denoted **a** by Thorsteinsson et al.[6] (*vide infra*) and which corresponds directly to the solution described by Gerratt et al..[1] We found in the present work that certain symmetry relations amongst the active orbitals appeared spontaneously during the optimization of our frozen-core SCGVB(**a**) wave function for $S_2N_2$, such that orbitals $\pi_3$ and $\pi_4$ can be generated from $\pi_1$ and $\pi_2$, respectively, by reflection in the $\sigma_{xz}$ mirror plane, whereas $\pi_6$ can be generated from $\pi_5$ by reflection in the $\sigma_{yz}$ mirror plane. Spontaneity of this type is usually a good indication of wave function stability with respect to breaking spatial symmetry. Other symmetry properties of the active orbitals, such as the invariance of $\pi_1$ and $\pi_2$ to reflection in the $\sigma_{yz}$ mirror plane and of $\pi_5$ to reflection in the $\sigma_{xz}$ mirror plane, also arose spontaneously. The symmetry-unique active orbitals $\pi_1$, $\pi_2$ and $\pi_5$, as depicted in the top row of Figure 3, clearly include a three-center SNS function that potentially makes it relatively difficult to interpret this wave function directly and unambiguously in terms of the sorts of VB structures that are shown in Figure 1. Nonetheless, Gerratt et al.[1] used the forms of such SCGVB orbitals, together with the pattern of active-space spin coupling, to assert the dominance of SS singlet diradical character. As was mentioned in the Introduction, such an interpretation is clearly at odds with the BOVB work of Braïda et al..[2] Indeed, those authors were able to use mostly qualitative arguments, stripping away 'delocalization tails', in order to suggest that the SCGVB wave function of Gerratt et al.[1] could in fact be more consistent with the NN singlet diradical character that was observed in BOVB calculations than with the original claim of SS singlet diradical character.

«Figure 3 near here»

We use here a robust numerical approach to establish the links between various SCGVB wave functions and BOVB descriptions. For this purpose, we turn now to our BOVB results, carried out with the same basis set and with the same choice of frozen core as our SCGVB calculations, so that we may compare like with like. Examining our frozen-core BOVB results, it can clearly be seen from Table 1 that the single BOVB structure with the lowest energy is structure **1** (see Figure 1), whether we take the active orbitals directly from the BOVB wave function or perform further separate

optimizations for each structure. On the other hand, the Chirgwin-Coulson weight of structure **1** in the BOVB wave function turns out to be just 30.1% (see top row of values in Table 2), so that it corresponds to a minority of the total wave function. A somewhat lower energy is given by the symmetry-determined linear combination of the four symmetry-equivalent structures **3-6**, with a Chirgwin-Coulson weight of 59.0%. These various findings are on the whole rather similar to those reported by Braïda et al.[2] and the general conclusions also turn out to be much the same from our corresponding frozen-core S-BOVB calculations (see Tables S4 and S6 in the Supporting Information). Additionally, the patterns of weights obtained with the Gallup-Norbeck scheme (see Tables S3 and S6 in the Supporting Information) are much the same as those from the Chirgwin-Coulson definition.

Whereas it is certainly true that structure **1** is indeed the most important one in our BOVB or S-BOVB wave functions, the majority of each of those wave functions is instead associated with the symmetry-determined linear combination ($\Phi_{3\text{-}6}$) of the four symmetry-equivalent structures **3-6**. Clearly, though, the interpretation put forward by Gerratt et al.,[1] based on claims of dominant SS singlet diradical character in their SCGVB wave function, remains distinctly anomalous. With this in mind, it proves to be very informative to use a fairly simple but robust numerical approach, that we now outline, to project the compact SCGVB(**a**) solution (based on just a single product of active orbitals) onto the corresponding BOVB representation.

In general terms, we wish to consider the expansion of a normalized wave function $\Psi$ in the following form:

$$\Psi = d_1\Phi_1 + d_2\Phi_2 + d_{3\text{-}6}\Phi_{3\text{-}6} + d_X\Phi_X \tag{5}$$

in which $\Phi_X$ is envisaged as a $\Psi$-dependent normalized entity which is orthogonal to each of the normalized BOVB structures $\Phi_1$, $\Phi_2$ and $\Phi_{3\text{-}6}$. It follows that:

$$\begin{pmatrix} \langle\Phi_1|\Psi\rangle \\ \langle\Phi_2|\Psi\rangle \\ \langle\Phi_{3\text{-}6}|\Psi\rangle \end{pmatrix} = \begin{pmatrix} 1 & \langle\Phi_1|\Phi_2\rangle & \langle\Phi_1|\Phi_{3\text{-}6}\rangle \\ \langle\Phi_1|\Phi_2\rangle & 1 & \langle\Phi_2|\Phi_{3\text{-}6}\rangle \\ \langle\Phi_1|\Phi_{3\text{-}6}\rangle & \langle\Phi_2|\Phi_{3\text{-}6}\rangle & 1 \end{pmatrix} \begin{pmatrix} d_1 \\ d_2 \\ d_{3\text{-}6} \end{pmatrix} \tag{6}$$

and so, given that we can calculate all of the overlap integrals that appear in eq 6 (see Tables S2 and S5 in the Supporting Information), it is very straightforward to solve for $d_1$, $d_2$ and $d_{3\text{-}6}$, and then to compute the Chirgwin-Coulson weights $W_k$. The corresponding weight in $\Psi$ of the normalized orthogonal complement $\Phi_X$, i.e. $W_X = d_X{}^2$, is most simply obtained from the requirement that the Chirgwin-Coulson weights must sum to unity. (This does of course correspond exactly to determining $d_X$ using the normalization condition for $\Psi$.) Our overall scheme is entirely equivalent to the application of a projection operator $\mathcal{P}$, defined according to:

$$\mathcal{P} = \sum_{k,l} |\Phi_k\rangle (\varDelta^{-1})_{kl} \langle \Phi_l| \qquad (k, l = 1, 2, 3\text{-}6) \qquad (7)$$

in which $\varDelta$ is the 3×3 overlap matrix shown in eq 6. The $\Psi$-dependent orthogonal complement, which we have chosen here to denote as $d_X \Phi_X$, is then simply $(1 - \mathcal{P})\Psi$.

Using the scheme that we have just described, the projection of the SCGVB(**a**) solution onto the basis of BOVB structures leads to the Chirgwin-Coulson weights that are reported in the second row of values in Table 2. The interpretation put forward by Gerratt et al.[1] does indeed turn out to be erroneous given that the single most important BOVB structure in SCGVB(**a**) is clearly **1**, albeit with a weight that is slightly lower than in our total BOVB wave function, with BOVB structure **2** (corresponding to SS singlet diradical character) being far less important. Just as we observed for the total BOVB wave function, it is the symmetry-determined linear combination of the four symmetry-equivalent BOVB structures **3-6**, with a Chirgwin-Coulson weight of 56.7%, which accounts for more than a half of the SCGVB(**a**) wave function. We find that the normalized orthogonal complement ($\Phi_X$), *i.e.* the part of the SCGVB(**a**) solution that is not described by this set of BOVB structures, has a weight of just 5.0%. (All of our key observations are much the same when using Gallup-Norbeck weights and/or if we project instead onto S-BOVB structures – see Tables S3, S4 and S6 in the Supporting Information.)

We now return to the observation of Thorsteinsson et al.[6] that there can exist rival SCGVB-like solutions that are fairly close in energy to SCGVB(**a**). Whereas the SCGVB(**a**) active orbitals span $3\times B_{1u}+1\times B_{2g}+2\times B_{3g}+0\times A_u$, which we may abbreviate to **a**=[3,1,2,0], Thorsteinsson et al.[6] suggested that there are various energetically nearby solutions which span various alternative distributions, including **b**=[3,2,1,0] and **c**=[2,1,2,1]. We find that the corresponding CASSCF(6,6) energies for active spaces **a** and **c** (see Table S1 in the Supporting Information) are particularly close to one another (differing by less than 0.35 millihartree), with the CASSCF(6,6) energy for active space **b** being inferior by 8.4 millihartree. In order to optimize the corresponding SCGVB(**b**) wave function, without it returning to the SCGVB(**a**) solution, we imposed the following constraints on the active orbitals: $\pi_3 = \hat{\sigma}_{yz}\pi_1$, $\pi_4 = \hat{\sigma}_{yz}\pi_2$ and $\pi_6 = \hat{\sigma}_{xz}\pi_5$. Other symmetry properties of the active orbitals, such as the invariance of $\pi_1$ and $\pi_2$ to reflection in the $\sigma_{xz}$ mirror plane and of $\pi_5$ to reflection in the $\sigma_{yz}$ mirror plane, arose spontaneously during the optimization. To a large extent, the resulting symmetry-unique active orbitals $\pi_1$, $\pi_2$ and $\pi_5$ for the SCGVB(**b**) solution (shown in the middle row of Figure 3) are somewhat reminiscent of those for SCGVB(**a**), except that the symmetry-unique three-center active orbital is now over NSN rather than SNS and it exhibits a larger contribution from the central atom of the triad. Just as we might have anticipated from the corresponding CASSCF(6,6)

7

energies, the SCGVB(**b**) solution is indeed energetically inferior to SCGVB(**a**), with the difference being 8.8 millihartree (see Table 3).

It proves to be especially informative to consider the projection of this SCGVB(**b**) solution onto the BOVB basis because the resulting Chirgwin-Coulson weights, as reported in Table 2, turn out to be fairly similar to those that we have described above for SCGVB(**a**). In spite of the differences in the forms and, particularly, the locations of the three-center active orbitals, these two wave functions do in fact turn out to be rather similar in terms of their BOVB character. Furthermore the overlap between the total SCGVB(**a**) and SCGVB(**b**) wave functions is 99.3% (see Table S8 in the Supporting Information) even though the overlap between the two normalized orthogonal complements ($\Phi_X$) is a little lower (86.1%, see Table S8 in the Supporting Information). All of this apparent numerical similarity between the SCGVB(**a**) and SCGVB(**b**) solutions (except for their different energies) reinforces our suspicion that one can easily be misled about the degree of (say) SS or NN singlet diradical character when relying mostly on the visual inspection of SCGVB active orbitals that are not sufficiently well localized. It does now appear that Gerratt et al.[1] were misdirected in this way when (mis)interpreting their SCGVB(**a**) wave function in terms of dominant SS singlet diradical character. (As before, all of our key observations are much the same when using Gallup-Norbeck weights and/or if we project instead onto S-BOVB structures.)

When restricting SCGVB active orbitals to span particular active spaces, Thorsteinsson et al.[6] found in some cases, such as **c**=[2,1,2,1], that the resulting SCGVB solution was symmetry broken. The proper full symmetry could be restored by using a two-configuration description in which the two sets of active orbitals were related by a particular $D_{2h}$ symmetry operation, such as a reflection or a rotation. With this in mind, we chose here to carry out two-configuration SCGVB calculations using the GMCSC program. Even without specifying any symmetry constraints between the two orbital strings, we observed convergence to a symmetry-pure solution in which the two sets of active orbitals are related to one another by reflection in the $\sigma_{yz}$ mirror plane. Additional symmetry relations emerged spontaneously within the two orbital strings, so that $\pi_3$, $\pi_4$ and $\pi_6$ can be generated from $\pi_1$, $\pi_2$ and $\pi_5$, respectively, by a $\hat{C}_2(z)$ rotation. (Specific details of these orbitals are slightly different from some of those envisaged by Thorsteinsson et al.[6] for their 'projected' **c** solution, prompting us to use a slightly different label.) The resulting energy for our variationally-optimized solution, which we label SCGVB($\mathbf{C_1} \oplus \mathbf{C_2}$), or SCGVB(**C**) for short, is somewhat better than that of SCGVB(**a**) (see Table 3), but the two sets of Chirgwin-Coulson weights (see Table 2) are fairly similar. Furthermore, the overlap between the total SCGVB(**a**) and SCGVB(**C**) wave functions is 99.4% (see Table S8 in the Supporting Information), with the overlap between the two normalized

orthogonal complements ($\varPhi_X$) being a little lower (88.2%, see Table S8 in the Supporting Information). The symmetry-unique active orbitals $\pi_1$, $\pi_2$ and $\pi_5$ for the SCGVB(**C**) solution, shown in the bottom row of Figure 3, clearly all exhibit a significant degree of (at least) two-center character, rendering it somewhat difficult to interpret them directly and unambiguously in terms of relative contributions from the sorts of VB structures shown in Figure 1. Relying instead on the projection onto BOVB structures, we can say that the largest net contributor (57.3%) is the symmetry-determined linear combination ($\varPhi_{3\text{-}6}$) of the four symmetry-equivalent BOVB structures **3-6**.

Just as there are CASSCF(6,6) solutions based on active spaces **e**=[3,1,1,1] and **f**=[2,2,2,0] which lie lower than that for **b**=[3,2,1,0] by *ca.* 3.0 and 1.6 millihartree, respectively (see Table S1 in the Supporting Information), it also proved possible to locate another single-configuration SCGVB solution which lies lower than SCGVB(**b**) by *ca.* 2.3 millihartree. However, given the dominance of SCGVB(**a**) and SCGVB(**C**) we decided not to pursue this solution, or any of the higher lying ones, in any detail.

The close proximity in energy of different SCGVB solutions, especially **a** and **C**, prompted us to wonder which of them would dominate variationally-optimized combinations of them. Accordingly, we also considered a VBCI(**a** ⊕ **b** ⊕ **C**) description, in which we combined the SCGVB(**a**), SCGVB(**b**) and SCGVB(**C**) wave functions via a nonorthogonal CI calculation, without relaxing any of the active-space spin-coupling coefficients. As can be seen from Table 3, this multicomponent wave function gives only a very modest energy improvement over SCGVB(**C**), with the **C** component remaining overwhelmingly dominant (94.2%). Projection of VBCI(**a** ⊕ **b** ⊕ **C**) onto the basis of BOVB structures gives weights that are very similar to those for SCGVB(**C**). Analogous outcomes are observed for the overlap between the VBCI(**a** ⊕ **b** ⊕ **C**) and SCGVB(**C**) wave functions, as well as for the overlap between the two orthogonal components, $\varPhi_X$ (see Tables S8 and S9 in the Supporting Information). Relaxing the various spin-coupling coefficients (without reoptimizing the active orbitals) produced only a very small energy lowering. All in all, other than making the resulting description more difficult to interpret directly, rather little is achieved by this mixing of the SCGVB(**a**), SCGVB(**b**) and SCGVB(**C**) wave functions.

The outcome is somewhat better, at least in terms of the total energy, if all of the active orbitals and active-space spin-coupling coefficients are simultaneously reoptimized (albeit with a limited number of suitable constraints so as to retain some distinction between the **a**, **b** and **C** components). We use the label GMCSC(**a** ⊕ **b** ⊕ **C**) for the resulting description. We observe from Table 3 that the reoptimized **C** component remains the largest contributor, but nearly 45% of the total is now due to the reoptimized **a** and **b** components. These changes to the weights of the different components of

GMCSC($\mathbf{a} \oplus \mathbf{b} \oplus \mathbf{C}$) relative to those of VBCI($\mathbf{a} \oplus \mathbf{b} \oplus \mathbf{C}$), as well as the lowering of the total energy, are accompanied by relatively small changes to the forms of the various symmetry-unique SCGVB active orbitals (see Figure S1 in the Supporting Information).

Projection of GMCSC($\mathbf{a} \oplus \mathbf{b} \oplus \mathbf{C}$) onto the basis of BOVB structures produces weights that are not so different from those for our various other SCGVB descriptions (see Table 2). As before, BOVB structure **1** (corresponding to NN singlet diradical character) is found to be more important than BOVB structure **2** (SS singlet diradical character), but the largest contribution (58.5%) comes from the symmetry-determined linear combination of the four symmetry-equivalent BOVB structures **3-6**, with no obvious diradical character. A further 4.9% is due to the normalized orthogonal complement ($\varPhi_X$). (We find again that all of our key observations are much the same when using Gallup-Norbeck weights instead of those from the Chirgwin-Coulson scheme and/or if we project instead onto S-BOVB structures.)

There are substantial differences between existing estimates of the degree of diradical character in the singlet ground state of $S_2N_2$, but it is important to note in this context, as was emphasized by Braïda et al.,[2] that significant singlet diradical character can co-exist with aromaticity in this molecule. At one extreme, Jung et al.[5] argued that $S_2N_2$ should be regarded as a $2\pi$-electron aromatic system, without any significant diradical character. Tuononen et al.[4] used a simple scheme this is based on the ratio of two CI coefficients in their CASSCF(22,16) description to estimate just 6% diradical character for this molecule. On the other hand, for the same CASSCF(22,16) wave function, they also considered a different form of analysis, based on idealized $p_\pi$ orbitals, which assigned a weight of 34% for **1** and of 14% for **2**.[4] The BOVB calculations of Braïda et al.,[2] as well as our own BOVB and S-BOVB calculations, also suggest significant weights for these two diradical structures, with **1** being somewhat more important than **2**, just as was found by Harcourt[3] when using a somewhat different VB approach.

Whereas Gerratt et al.[1] (mis)interpreted their $S_2N_2$ wave function in terms of dominant SS singlet diradical character, our projection of the SCGVB(**a**) description onto BOVB structures reveals a higher weight for **1** than for **2**. Indeed, all of our projections of SCGVB-like wave functions for $S_2N_2$ onto the basis of BOVB or S-BOVB structures (and an orthogonal complement) show **1** to be more important than **2**, but they also indicate that nearly 60% of the wave function is instead associated with the symmetry-determined linear combination of the four symmetry-equivalent BOVB structures **3-6**. This relatively high combined weight for structures **3-6** is of course consistent with the well-established pattern for the atomic charges in which nitrogen is negative and sulfur is positive.[5] We find that the net QTAIM charges for the SCGVB(**a**) total electron density are numerically much the

same as those just for the valence $\pi$ space. This suggests that inferences about the bonding in the valence $\pi$ system from considerations of the overall charge distribution, such as those discussed by Jung et al.,[5] are not skewed by any significant charge separation in the $\sigma$-bonded framework. (Our QTAIM charges for SCGVB(**a**) do of course have the correct NS polarity. We also find that the QTAIM charges for the GMCSC(**a** $\oplus$ **b** $\oplus$ **C**) total electron density are very similar to those for SCGVB(**a**).)

**3.2. $S_4N_4^{2+}$.** We find that free optimization of a single-configuration SCGVB wave function for $S_4N_4^{2+}$ results in a solution that corresponds to one of the $D_{2h}$ subgroups of the full molecular point group ($D_{4h}$). Amongst many other deviations from full $D_{4h}$ symmetry, such that the desired $^1A_{1g}$ wave function has a small but not negligible $^1B_{2g}$ contaminant, we observed that active orbitals $\pi_1$ and $\pi_2$ were each relatively close to being invariant under reflection in the $\sigma_{yz}$ mirror plane, but they were not exactly so. The various findings described above for $S_2N_2$ are suggestive that a suitable way forward would be to optimize a two-configuration SCGVB description in which the two sets of active orbitals are related to one another by an appropriate reflection or rotation. We label the resulting wave function as SCGVB(**A₁** $\oplus$ **A₂**), or SCGVB(**A**) for short. Nonetheless we also consider a single-configuration SCGVB description in which the active orbitals are suitably constrained so as to ensure that the resulting wave function, which we denote SCGVB(**B**), still respects the full $D_{4h}$ symmetry.

We found at convergence of our symmetry-pure SCGVB(**A**) solution that the two sets of active orbitals (*i.e.* those for **A₁** and **A₂**) are related to one another by reflection in the $\sigma_{xz}$ mirror plane. Additionally, we observed symmetry relations within each orbital string, such that reflection of $\pi_1$ and $\pi_2$ in the plane $x = y$ yields $\pi_3$ and $\pi_4$, respectively, and $\hat{C}_2(z)$ rotation of $\pi_1$ and $\pi_2$ gives $\pi_5$ and $\pi_6$, respectively. Similarly, reflection of $\pi_1$, $\pi_2$ and $\pi_9$ in the plane $x = -y$ yields $\pi_7$, $\pi_8$ and $\pi_{10}$, respectively. For the optimization of the SCGVB(**B**) solution, we constrained active orbitals $\pi_1$ and $\pi_2$ to be exactly $\hat{\sigma}_{yz}$ invariant and it also proved necessary to add as constraints symmetry relations for $\pi_3$-$\pi_8$ which emerged spontaneously for SCGVB(**A**). Additionally, after some experimentation in which we sought the lowest possible energy, we found that we had to constrain $\pi_9$ for SCGVB(**B**) to be invariant under reflection in the plane $x = y$ as well as under $\hat{C}_2(z)$ rotation, with $\pi_{10}$ generated from $\pi_9$ by a $\hat{C}_4(z)$ rotation.

«Figure 4 near here»

The resulting symmetry-unique active orbitals $\pi_1$, $\pi_2$ and $\pi_9$ from the SCGVB(**A**) and SCGVB(**B**) calculations are displayed in the top and bottom rows, respectively, of Figure 4. Except for being more localized, the SCGVB(**A**) active orbitals are fairly reminiscent of those for the $S_2N_2$ SCGVB(**C**) solution (bottom row of Figure 3). On the other hand, the symmetry-unique SCGVB(**B**)

active orbitals include a three-center SNS function, just as was the case for the $S_2N_2$ SCGVB(**a**) solution (top row of Figure 3). As can be seen from Table 4, solution SCGVB(**A**) lies somewhat lower than SCGVB(**B**), as we should have expected. Computing the energy of the **A₁** (or **A₂**) component using the same active orbitals and spin-coupling coefficients as in the SCGVB(**A**) solution, we find that the energy lowering associated with mixing together these **A₁** and **A₂** components is 160 kJ/mol (38 kcal/mol). The corresponding energy change from **C₁** to SCGVB(**C**) in the case of $S_2N_2$ is 124 kJ/mol (30 kcal/mol). In both cases, the optimization of the active orbitals allows the two configurations to become more different from one another, at the expense of the energy of each of them separately, with the consequence that the mixing of the two components corresponds to a significant energy lowering. (Additional data are available in Table S10 in the Supporting Information.)

In keeping with our experience for $S_2N_2$, combining the SCGVB(**A**) and SCGVB(**B**) descriptions of $S_4N_4{}^{2+}$ via a nonorthogonal CI calculation, thereby generating the VBCI(**A** ⊕ **B**) wave function (without relaxing any of the active-space spin-coupling coefficients), results in relatively little energy improvement, with SCGVB(**A**) remaining dominant (see Table 4). Just as was the case for the VBCI(**a** ⊕ **b** ⊕ **C**) description of $S_2N_2$, relaxation of the various spin-coupling coefficients, without reoptimizing the active orbitals, produced only a very small energy lowering. Larger changes are achieved for GMCSC(**A** ⊕ **B**), in which all of the active orbitals and active-space spin-coupling coefficients are simultaneously reoptimized (subject to a limited number of suitable constraints so as to retain some distinction between the **A** and **B** components). The reoptimized **A** component remains the largest contributor and there are only relatively small changes to the forms of the various symmetry-unique SCGVB active orbitals (see Figure S2 in the Supporting Information). Amongst other changes from VBCI(**A** ⊕ **B**) to GMCSC(**A** ⊕ **B**), the $\langle A_1|A_2\rangle$ overlap is reduced from 0.675 to 0.571 whereas $\langle A|B\rangle$ goes down from 0.951 to 0.847 (see Table S11 in the Supporting Information).

## 4. SUMMARY AND CONCLUSIONS

As has been shown before,[6] $S_2N_2$ <mark>at its idealized square geometry, close to experiment,</mark> offers multiple energetically close $\pi$-space '6 electrons in 6 orbitals' CASSCF solutions and thus also various competing SCGVB descriptions. Although the active space $2\times B_{1u}+1\times B_{2g}+2\times B_{3g}+1\times A_u$, or **c**=[2,1,2,1] for short, gives the lowest CASSCF(6,6) energy for the calculations carried out here, the corresponding **a**=[3,1,2,0] solution lies less than 0.35 millihartree higher. (The ordering of these two solutions was reversed in the calculations of Thorsteinsson et al.,[6] who used a somewhat smaller basis set) We find that the energetically preferred single-configuration SCGVB wave function is related to active space **a**. This SCGVB(**a**) solution, which corresponds to the one described by Gerratt at al.,[1]

appears at first sight of the orbitals and active-space total spin function to correspond to dominant SS singlet diradical character. Somewhat higher in energy is a single-configuration SCGVB(**b**) solution, which appears at first sight to be dominated by NN singlet diradical character. As was pointed out by Thorsteinsson et al.,[6] the occurrence of negative overlaps for the SS and NN singlet diradical orbital pairs, with nodal planes between the two participating centers, means that there can be no question of any cross-ring bonding in either of the SCGVB(**a**) or SCGVB(**b**) descriptions. Given the occurrence of three-center orbitals in both descriptions, as well as delocalization tails, it is of course easy to be misdirected by an examination of the shapes and locations of such active orbitals. In reality, in spite of featuring active orbitals that are visually somewhat different, these two SCGVB solutions turn out to be rather similar to one another (except in terms of their total energies).

The corresponding single-configuration SCGVB wave function for $S_2N_2$ active space **c** is symmetry broken and so we optimized instead a two-configuration SCGVB wave function, which we label SCGVB(**C**). (Specific details of the two orbital strings are slightly different from some of those envisaged by Thorsteinsson et al.[6] for their 'projected' **c** solution, prompting us to use a slightly different label.) Although our variationally-optimized SCGVB(**C**) solution turns out to be energetically preferred over SCGVB(**a**) by more than 12 millihartree, it is still reasonable to wonder whether **C** would dominate a variationally-optimized combination. A nonorthogonal CI with fixed active orbitals and fixed spin-coupling coefficients, VBCI(**a** ⊕ **b** ⊕ **C**), produced rather little energy improvement over SCGVB(**C**), with **C** being by far the dominant component. Subsequent relaxation of the spin-coupling coefficients achieved relatively little for the energy whereas simultaneous reoptimization also of the active orbitals, in the GMCSC(**a** ⊕ **b** ⊕ **C**) description, yielded a modest energy improvement of *ca*. 9.5 millihartree. Nonetheless, although the reoptimized **a** and **b** components collectively account for nearly 45% of the total GMCSC(**a** ⊕ **b** ⊕ **C**) wave function, the largest contribution is due to the reoptimized **C** component.

Subsequent calculations for the 10-electron $\pi$ space of the $D_{4h}$ $S_4N_4^{2+}$ ring produced a symmetry-broken single-configuration SCGVB solution, unless suitable constraints were placed on the orbitals, as was done for our SCGVB(**B**) description. Our optimal two-configuration solution, which we label SCGVB(**A**), turns out to be energetically preferred over SCGVB(**B**) by nearly 51 millihartree. Whereas the symmetry-unique SCGVB(**B**) active orbitals are found to include a three-center SNS function, just as was the case for the $S_2N_2$ SCGVB(**a**) solution, the SCGVB(**A**) active orbitals are more reminiscent of those for the $S_2N_2$ SCGVB(**C**) solution, except for being more localized. We found that the mixing of SCGVB(**A**) and SCGVB(**B**) generates hardly any energy improvement unless the active orbitals and the spin-coupling are simultaneously reoptimized. The resulting

GMCSC($\mathbf{A} \oplus \mathbf{B}$) solutions lies lower than SCGVB($\mathbf{A}$) by *ca*. 7 millihartree, with the reoptimized $\mathbf{A}$ component remaining the largest contributor.

For both of the $S_2N_2$ and $S_4N_4^{2+}$ rings at their idealized geometries, close to experiment, our preferred compact SCGVB description of the $\pi$-electron system is provided by the variational optimization of two configurations which turn out to be symmetry related to one another. The optimization instead of symmetry-pure single-configuration SCGVB wave functions leads to the involvement of three-center SNS or NSN orbitals, which now seems to be an unnecessary complication. In neither ring system is very much achieved from the mixing of such competing solutions.

As is to be expected, our BOVB and S-BOVB calculations for $S_2N_2$ confirm that structure **1** (corresponding to NN singlet diradical character) is more important than structure **2** (corresponding to SS singlet diradical character),[2,3,4] but the largest contribution (*ca*. 60%) turns out to be due to the symmetry-determined linear combination of the four symmetry-equivalent structures **3**-**6**, with no obvious diradical character. Much the same pattern was consistently found when we used a simple but robust projection of our various SCGVB wave functions for $S_2N_2$ onto the basis of BOVB or S-BOVB structures (plus an orthogonal complement). In particular, it does indeed now appear that Gerratt et al.[1] were misdirected by active orbitals that are not sufficiently localized when (mis)interpreting their SCGVB(**a**) wave function in terms of dominant SS singlet diradical character.

## ■ ASSOCIATED CONTENT

### Supporting Information

The Supporting Information is available free of charge on the ACS Publications website at DOI: 10.1021/acs.jpca.xxx.

Various additional numerical results (including energies, overlaps and weights) and orbital depictions for $S_2N_2$ and $S_4N_4^{2+}$.

## ■ AUTHOR INFORMATION

### Corresponding Author

*E-mail: dlc@liverpool.ac.uk

### Notes

The authors declare no competing financial interest.

## ■ REFERENCES

1. Gerratt, J.; McNicholas, S. J.; Karadakov, P. B.; Sironi, M.; Raimondi, M.; Cooper, D. L., The extraordinary electronic structure of $N_2S_2$. *J. Am. Chem. Soc.* **1996,** *118* (27), 6472-6476.

2. Braïda, B.; Lo, A.; Hiberty, P. C., Can Aromaticity Coexist with Diradical Character? An Ab Initio Valence Bond Study of $S_2N_2$ and Related $6\pi$-Electron Four-Membered Rings $E_2N_2$ and $E_4^{2+}$ (E=S, Se, Te). *ChemPhysChem* **2012,** *13* (3), 811-819.

3. Harcourt, R. D., Notes on Valence Bond Structures for $S_2N_2$ and Related Systems. *ChemPhysChem* **2013,** *14* (12), 2859-2864.

4. (a) Tuononen, H. M.; Suontamo, R.; Valkonen, J.; Laitinen, R. S., Electronic structures and spectroscopic properties of $6\pi$-electron ring molecules and ions $E_2N_2$ and $E_4^{2+}$ (E = S, Se, Te). *J. Phys. Chem. A* **2004,** *108* (26), 5670-5677; (b) Tuononen, H. M.; Suontamo, R.; Valkonen, J.; Laitinen, R. S.; Chivers, T., Electronic Structures and Molecular Properties of Chalcogen Nitrates $Se_2N_2$ and $SeSN_2$. *J. Phys. Chem. A* **2005,** *109* (28), 6309-6317.

5. Jung, Y.; Heine, T.; Schleyer, P. v. R.; Head-Gordon, M., Aromaticity of four-membered-ring $6\pi$-electron systems: $N_2S_2$ and $Li_2C_4H_4$. *J. Am. Chem. Soc.* **2004,** *126* (10), 3132-3138.

6. Thorsteinsson, T.; Cooper, D. L., Nonorthogonal weights of modern VB wavefunctions. Implementation and applications within CASVB. *J. Math. Chem.* **1998,** *23* (1-2), 105-126.

7. Cooper, D. L.; Karadakov, P. B., Spin-coupled descriptions of organic reactivity. *Int. Rev. Phys. Chem.* **2009,** *28* (2), 169-206.

8. Gerratt, J.; Lipscomb, W. N., Spin-coupled wave functions for atoms and molecules. *Proc. Natl. Acad. Sci. U. S. A.* **1968,** *59* (2), 332-335.

9. Ladner, R. C.; Goddard, W. A., Improved quantum theory of many-electron systems. V. The spin-coupling optimized GI method. *J. Chem. Phys.* **1969,** *51* (3), 1073-1087.

10. Gillespie, R. J.; Kent, J. P.; Sawyer, J. F.; Slim, D. R.; Tyrer, J. D., Reactions of $S_4N_4$ with $SbCl_5$, $SbF_5$, $AsF_5$, $PF_5$, and $HSO_3F$. Preparation and Crystal Structures of Salts of the $S_4N_4^{2+}$ Cation: $(S_4N_4)(Sb_3F_{14})(SbF_6)$, $(S_4N_4)(SO_3F)_2$, $(S_4N_4)(AsF_6)_2 \cdot SO_2$, $(S_4N_4)(AlCl_4)_2$, and $(S_4N_4)(SbCl_6)_2$. *Inorg. Chem.* **1981,** *20* (11), 3799-3812.

11. Chirgwin, B. H.; Coulson, C. A., The electronic structure of conjugated systems. VI. *Proc. R. Soc. London, A* **1950,** *201* (1065), 196-209.

12. Gallup, G. A.; Norbeck, J. M., Population analyses of valence-bond wavefunctions and $BeH_2$. *Chem. Phys. Lett.* **1973,** *21* (3), 495-500.

13. (a) Penotti, F. E., The optimized-basis-set multiconfiguration spin-coupled method for the ab initio calculation of atomic and molecular electronic wave functions. *Int. J. Quantum Chem.* **1993,** *46* (4), 535-576; (b) Penotti, F. E., Generalization of the optimized-basis-set multi-configuration spin-coupled method for the ab initio calculation of atomic and molecular electronic wave functions. *Int. J. Quantum Chem.* **1996,** *59* (5), 349-378; (c) Penotti, F. E., On the identification of symmetry-forbidden spin subspaces for configurations employing nonorthogonal orbitals. *Int. J. Quantum Chem.* **2000,** *78* (1), 24-31; (d) Penotti, F. E., Orbital-orthogonality constraints and basis-set optimization. *J. Comput. Chem.* **2006,** *27* (6), 762-772.

14. (a) Schmidt, M. W.; Baldridge, K. K.; Boatz, J. A.; Elbert, S. T.; Gordon, M. S.; Jensen, J. H.; Koseki, S.; Matsunaga, N.; Nguyen, K. A.; Su, S. J.; Windus, T. L.; Dupuis, M.; Montgomery, J. A., General atomic and molecular electronic-structure system. *J. Comput. Chem.* **1993,** *14*

(11), 1347-1363; (b) Gordon, M. S.; Schmidt, M. W., *Advances in electronic structure theory: GAMESS a decade later*. 2005; p 1167-1189.

15. Schaftenaar, G.; Noordik, J. H., Molden: a pre- and post-processing program for molecular and electronic structures. *J. Comput. Aided Mol. Des.* **2000,** *14* (2), 123-134.

16. Bader, R. F. W., *Atoms in Molecules, A Quantum Theory*. Oxford University Press: Oxford, 1990.

17. Keith, T. A. *AIMAll (Version 17.01.25)*, TK Gristmill Software: Overland Park KS, USA, 2017; aim.tkgristmill.com.

18. (a) Werner, H.-J.; Knowles, P. J.; Knizia, G.; Manby, F. R.; Schütz, M., Molpro: a general-purpose quantum chemistry program package. *Wiley Interdisciplinary Reviews: Computational Molecular Science* **2012,** *2* (2), 242-253; (b) Werner, H.-J.; Knowles, P. J.; Knizia, G.; Manby, F. R.; Schütz, M.; Celani, P.; Györffy, W.; Kats, D.; Korona, T.; Lindh, R.; Mitrushenkov, A.; Rauhut, G.; Shamasundar, K. R.; Adler, T. B.; Amos, R. D.; Bernhardsson, A.; Berning, A.; Cooper, D. L.; Deegan, M. J. O.; Dobbyn, A. J.; Eckert, F.; Goll, E.; Hampel, C.; Hesselmann, A.; Hetzer, G.; Hrenar, T.; Jansen, G.; Köppl, C.; Liu, Y.; Lloyd, A. W.; Mata, R. A.; May, A. J.; McNicholas, S. J.; Meyer, W.; Mura, M. E.; Nicklass, A.; O'Neill, D. P.; Palmieri, P.; Peng, D.; Pflüger, K.; Pitzer, R.; Reiher, M.; Shiozaki, T.; Stoll, H.; Stone, A. J.; Tarroni, R.; Thorsteinsson, T.; Wang, M. *MOLPRO, version 2015.1, a package of ab initio programs*, Cardiff, UK, 2015; www.molpro.net.

**Figure 1.** Structures used in the BOVB calculations for $S_2N_2$.



**1**                    **2**                    **3-6**
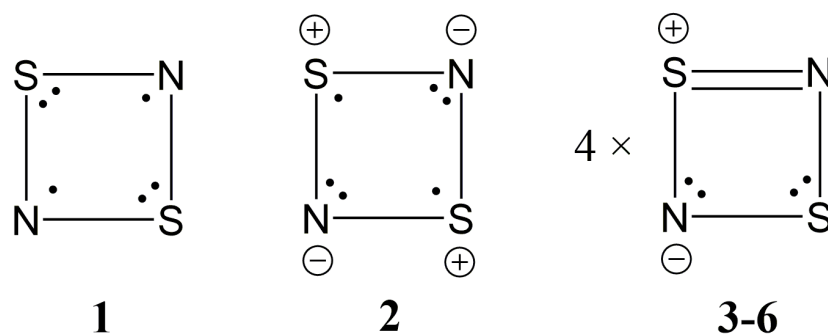
**Figure 2.** Geometries and orientation used for $S_2N_2$ and $S_4N_4^{2+}$.



17
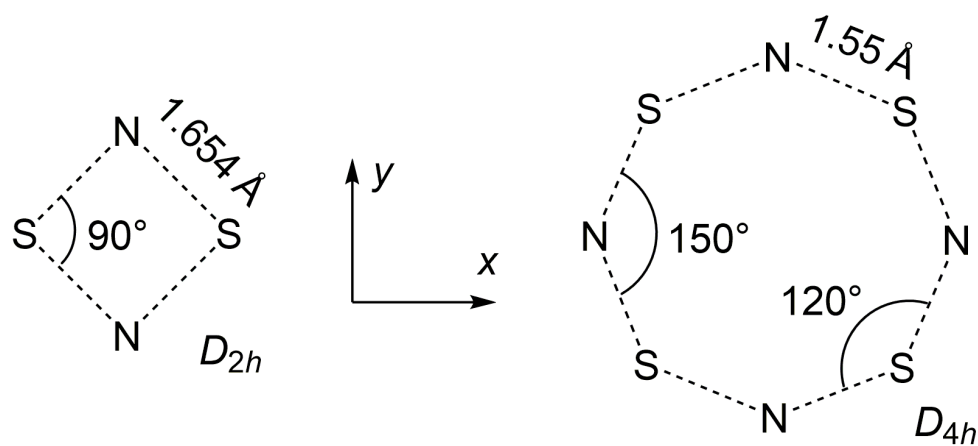
**Figure 3.** Symmetry-unique active orbitals $\pi_1$, $\pi_2$ and $\pi_5$ (left to right) for frozen-core $S_2N_2$ wave functions: SCGVB(**a**) (top row); SCGVB(**b**) (middle row); SCGVB(**C**) (bottom row).

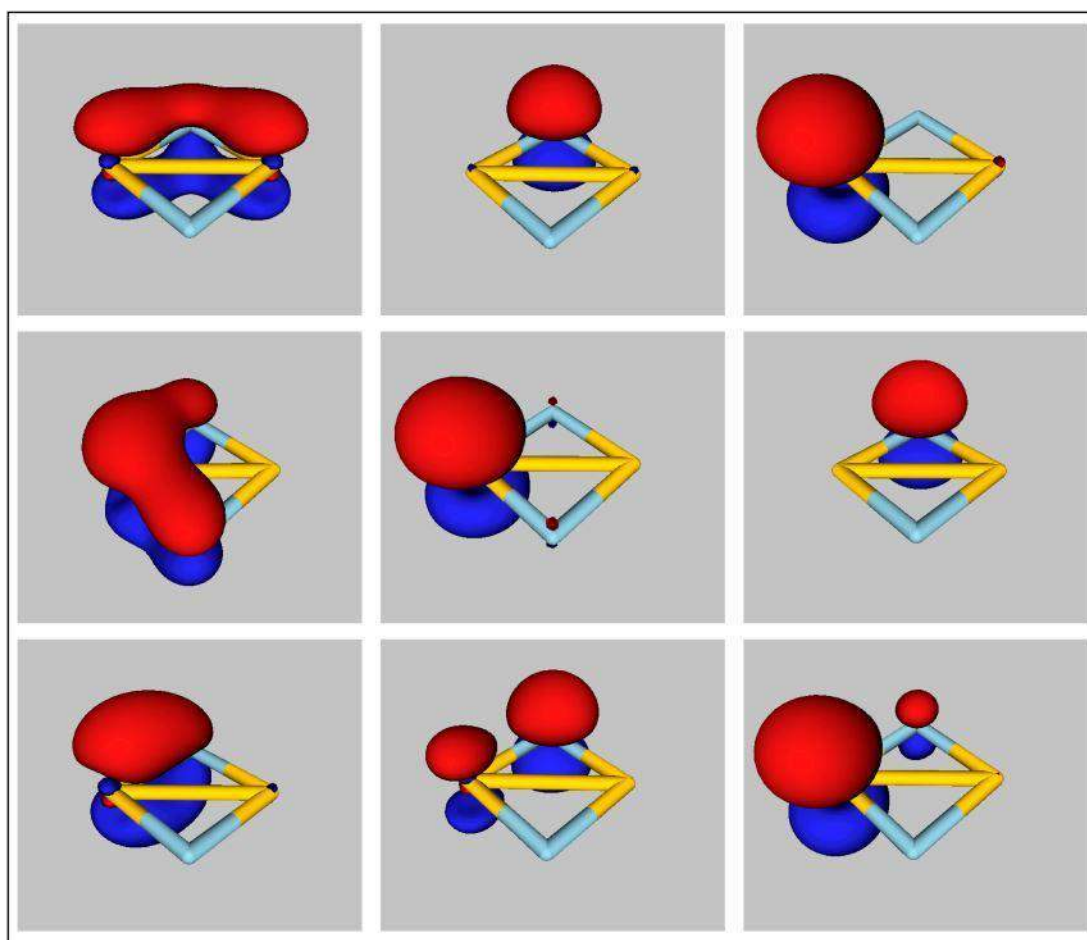**Figure 4.** Symmetry-unique active orbitals $\pi_1$, $\pi_2$ and $\pi_9$ (left to right) for frozen-core $S_4N_4^{2+}$ wave functions: SCGVB(**A**) (top row); SCGVB(**B**) (bottom row).
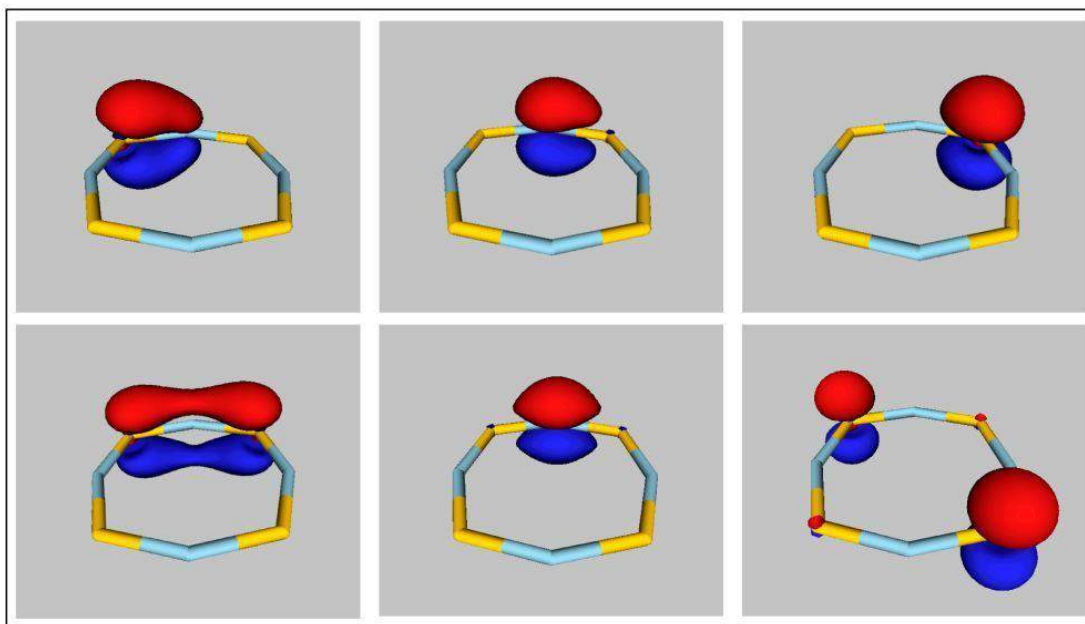
**Table 1. Energies (in hartree) from frozen-core six-structure BOVB calculations for $S_2N_2$. 'Fixed' signifies the use of active orbitals taken directly from the six-structure BOVB calculation, whereas 'Relaxed' signifies further optimization.**

| Structures | Fixed | Relaxed |
|:---:|:---:|:---:|
| **1** | -903.79363 | -903.81387 |
| **2** | -903.65901 | -903.69344 |
| **3** | -903.70564 | -903.71732 |
| **3-6** | -903.88008 | -903.88919 |
| **1-6** | -903.94635 | -903.94635 |

**Table 2. Chirgwin-Coulson weights, with structures 1 to 6 taken directly from the frozen-core six-structure BOVB calculations for $S_2N_2$ and where X signifies a normalized orthogonal complement.**

| Wave function | **1** | **2** | **3-6** | **X** |
|:---:|:---:|:---:|:---:|:---:|
| BOVB (**1-6**) | 30.1% | 10.9% | 59.0% | – |
| SCGVB(**a**) | 25.1% | 13.2% | 56.7% | 5.0% |
| SCGVB(**b**) | 27.1% | 13.0% | 54.7% | 5.2% |
| SCGVB(**C**) | 24.6% | 13.3% | 57.3% | 4.7% |
| VBCI(**a** ⊕ **b** ⊕ **C**) | 24.9% | 13.3% | 57.2% | 4.6% |
| GMCSC(**a** ⊕ **b** ⊕ **C**) | 24.6% | 12.0% | 58.5% | 4.9% |

**Table 3.** **Energies and Chirgwin-Coulson weights for (combinations of) frozen-core SCGVB wave functions for $S_2N_2$.**

| Wave function | Energy (hartree) | Weights a | b | C |
|---|---|---|---|---|
| SCGVB(**a**) | -903.98083 | 100% | – | – |
| SCGVB(**b**) | -903.97206 | – | 100% | – |
| SCGVB(**C**) | -903.99314 | – | – | 100% |
| VBCI(**a** $\oplus$ **b** $\oplus$ **C**) | -903.99326 | -2.1% | 7.9% | 94.2% |
| GMCSC(**a** $\oplus$ **b** $\oplus$ **C**) | -904.00270 | 25.9% | 19.0% | 55.1% |

**Table 4.** **Energies and Chirgwin-Coulson weights for (combinations of) frozen-core SCGVB wave functions for $S_4N_4^{2+}$.**

| Wave function | Energy (hartree) | Weights A | B |
|---|---|---|---|
| SCGVB(**A**) | -1807.29841 | 100% | – |
| SCGVB(**B**) | -1807.24746 | – | 100% |
| VBCI(**A** $\oplus$ **B**) | -1807.29856 | 95.1% | 4.9% |
| GMCSC(**A** $\oplus$ **B**) | -1807.30558 | 73.0% | 27.0% |

# Supporting Information

## Spin-Coupled Generalized Valence Bond (SCGVB) Descriptions of $\pi$-Electron Systems in $S_2N_2$ and $S_4N_4^{2+}$ Rings

Fabio E. Penotti,[†] David Cooper,*[‡] and Peter B. Karadakov[§]

[†]Consiglio Nazionale delle Ricerche, Istituto di Scienze e Tecnologie Molecolari, Via Golgi 19, I−20133 Milano MI, Italy

[‡]Department of Chemistry, University of Liverpool, Liverpool L69 7ZD, UK

[§]Department of Chemistry, University of York, Heslington, York YO10 5DD, UK

*E-mail: dlc@liverpool.ac.uk

## Contents

**Table S1.  Tests of different sets of CASSCF inactive orbitals for $S_2N_2$.**

*(a)  Spaces spanned*

|  | $B_{1u}$ | $B_{2g}$ | $B_{3g}$ | $A_u$ |  |
|---|---|---|---|---|---|
| $\pi$ full-valence (*fv*) | 2 | 1 | 1 | 0 | [2,1,1,0] |
| **a** | 3 | 1 | 2 | 0 | [3,1,2,0] |
| **b** | 3 | 2 | 1 | 0 | [3,2,1,0] |
| **c** | 2 | 1 | 2 | 1 | [2,1,2,1] |
| **d** | 2 | 2 | 1 | 1 | [2,2,1,1] |
| **e** | 3 | 1 | 1 | 1 | [3,1,1,1] |
| **f** | 2 | 2 | 2 | 0 | [2,2,2,0] |
| *max*(**a,b,c,d,e,f**) | 3 | 2 | 2 | 1 | [3,2,2,1] |

*(b)  CASSCF energies (in hartree) and selected differences (in millihartree) for different choices of inactive orbitals. ($E_{RHF}$ = -903.91753 hartree)*

| Inactive orbitals | Energy | | | | | | |
|---|---|---|---|---|---|---|---|
|  | *fv*=[2,1,1,0] | **a**=[3,1,2,0] | **b**=[3,2,1,0] | **c**=[2,1,2,1] | **max**=[3,2,2,1] | **a − c** | **b − c** |
| Variational | -903.96018 | -903.98159 | -903.97320 | -903.98194 | -903.99550 | 0.35 | 8.73 |
| *fv*=[2,1,1,0] | -903.96018 | -903.98140 | -903.97315 | -903.98190 | -903.99536 | 0.51 | 8.76 |
| **a**=[3,1,2,0] | -903.95998 | -903.98159 | -903.97314 | -903.98183 | -903.99548 | 0.24 | 8.69 |
| **b**=[3,2,1,0] | -903.96013 | -903.98152 | -903.97320 | -903.98192 | -903.99547 | 0.40 | 8.71 |
| **c**=[2,1,2,1] | -903.96015 | -903.98148 | -903.97319 | -903.98194 | -903.99545 | 0.46 | 8.75 |
| *max*=[3,2,2,1] | -903.96005 | -903.98157 | -903.97318 | -903.98189 | -903.99550 | 0.31 | 8.71 |

*(c)  Energies (in hartree) for additional CASSCF descriptions.*

| Inactive orbitals | Energy | | |
|---|---|---|---|
|  | **d**=[2,2,1,1] | **e**=[3,1,1,1] | **f**=[2,2,2,0] |
| variational | -903.97044 | -903.97614 | -903.97487 |
| *max*=[3,2,2,1] | -903.97032 | -903.97613 | -903.97483 |

**Figure S1.** Symmetry-unique active orbitals in the frozen-core GMCSC($\mathbf{a} \oplus \mathbf{b} \oplus \mathbf{C}$) wave function for $S_2N_2$. Orbitals shown in the same order as in Figure 3.
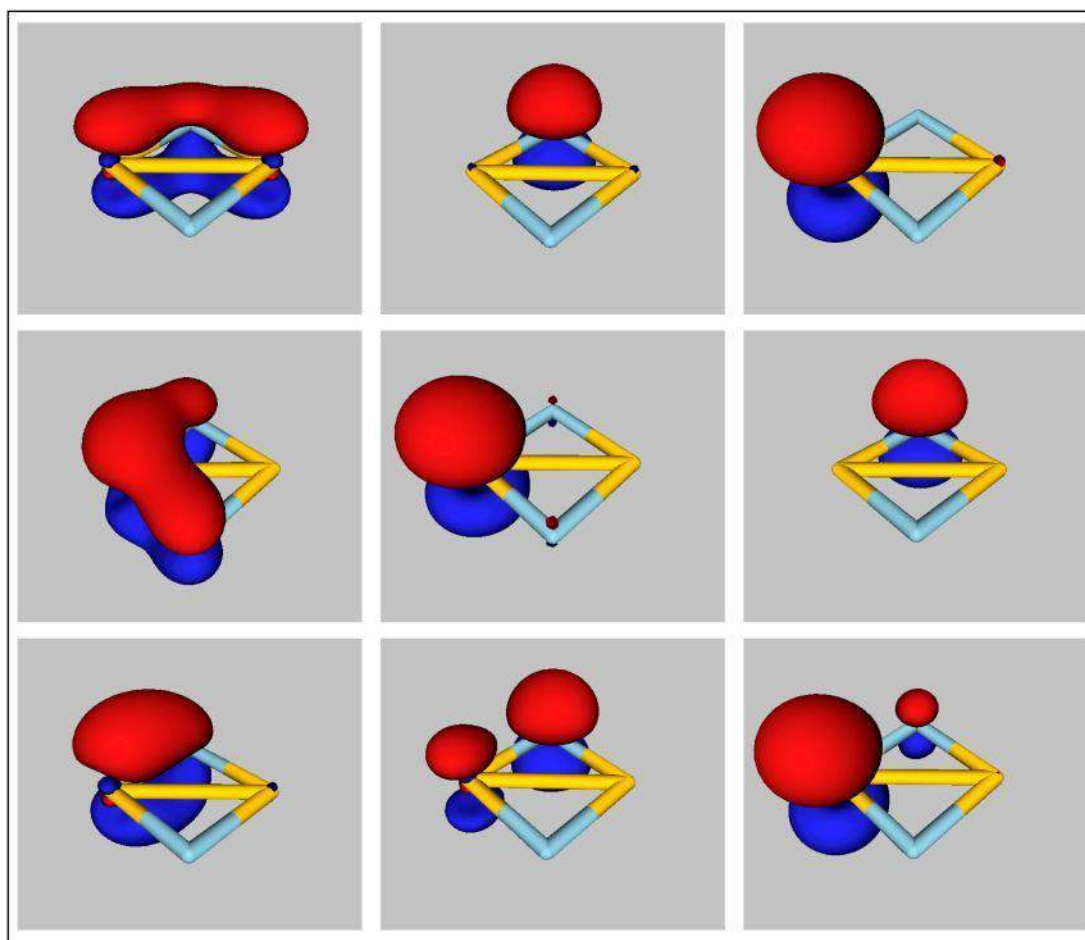


**Table S2.** **Overlap integrals for frozen-core six-structure BOVB wave functions for $S_2N_2$ (where X signifies a normalized orthogonal complement).**

|  | 1 | 2 | 3-6 |
|---|---|---|---|
| **1** | 1.000 | 0.130 | 0.472 |
| **2** | 0.130 | 1.000 | 0.475 |
| **3-6** | 0.472 | 0.475 | 1.000 |

|  | 1 | 2 | 3-6 | 1-6 | X |
|---|---|---|---|---|---|
| SCGVB($\mathbf{a}$) | 0.689 | 0.575 | 0.906 | 0.973 | 0.230 |
| SCGVB($\mathbf{b}$) | 0.703 | 0.568 | 0.899 | 0.973 | 0.230 |
| SCGVB($\mathbf{C}$) | 0.686 | 0.577 | 0.909 | 0.975 | 0.224 |
| VBCI($\mathbf{a} \oplus \mathbf{b} \oplus \mathbf{C}$) | 0.688 | 0.577 | 0.909 | 0.975 | 0.221 |
| GMCSC($\mathbf{a} \oplus \mathbf{b} \oplus \mathbf{C}$) | 0.688 | 0.564 | 0.912 | 0.974 | 0.288 |

**Table S3.** **Inverse-overlap (Gallup-Norbeck) weights, with 1 to 6 taken directly from the frozen-core six-structure BOVB calculations for $S_2N_2$ and where X signifies a normalized orthogonal complement.**

| Wave function | 1 | 2 | 3-6 | X |
|---|---|---|---|---|
| BOVB (**1-6**) | 31.8% | 7.4% | 60.8% | – |
| SCGVB(**a**) | 25.5% | 10.2% | 59.3% | 5.0% |
| SCGVB(**b**) | 28.7% | 10.1% | 56.0% | 5.2% |
| SCGVB(**C**) | 24.8% | 10.2% | 60.2% | 4.7% |
| VBCI(**a** ⊕ **b** ⊕ **C**) | 25.1% | 10.3% | 60.0% | 4.6% |
| GMCSC(**a** ⊕ **b** ⊕ **C**) | 24.5% | 8.6% | 62.0% | 4.9% |

**Table S4.** **Energies (in hartree) from frozen-core six-structure S-BOVB calculations for $S_2N_2$. 'Fixed' signifies the use of active orbitals taken directly from the six-structure S-BOVB calculation, whereas 'Relaxed' signifies further optimization.**

| Structures | Fixed | Relaxed |
|---|---|---|
| **1** | -903.79978 | -903.85801 |
| **2** | -903.66658 | -903.71685 |
| **3** | -903.71852 | -903.73523 |
| **3-6** | -903.89354 | -903.90623 |
| **1-6** | -903.96054 | -903.96054 |

**Table S5.** **Overlap integrals for frozen-core six-structure S-BOVB wave functions for $S_2N_2$ (where X signifies a normalized orthogonal complement).**

| | 1 | 2 | 3-6 |
|---|---|---|---|
| **1** | 1.000 | 0.136 | 0.471 |
| **2** | 0.136 | 1.000 | 0.469 |
| **3-6** | 0.471 | 0.469 | 1.000 |

| | 1 | 2 | 3-6 | 1-6 | X |
|---|---|---|---|---|---|
| SCGVB(**a**) | 0.685 | 0.575 | 0.905 | 0.972 | 0.235 |
| SCGVB(**b**) | 0.701 | 0.566 | 0.895 | 0.970 | 0.241 |
| SCGVB(**C**) | 0.683 | 0.577 | 0.910 | 0.975 | 0.223 |
| VBCI(**a** ⊕ **b** ⊕ **C**) | 0.685 | 0.577 | 0.909 | 0.975 | 0.221 |
| GMCSC(**a** ⊕ **b** ⊕ **C**) | 0.689 | 0.563 | 0.914 | 0.977 | 0.212 |

**Table S6.** **Chirgwin-Coulson and inverse-overlap weights, with 1 to 6 taken directly from the frozen-core six-structure S-BOVB calculations for $S_2N_2$ and where X signifies a normalized orthogonal complement.**

*(a) Chirgwin-Coulson weights*

| Wave function | 1 | 2 | 3-6 | X |
|---|---|---|---|---|
| S-BOVB (**1-6**) | 28.9% | 11.3% | 59.8% | – |
| SCGVB(**a**) | 24.5% | 13.4% | 56.8% | 5.4% |
| SCGVB(**b**) | 26.9% | 13.0% | 54.4% | 5.7% |
| SCGVB(**C**) | 24.1% | 13.3% | 57.8% | 4.8% |
| VBCI(**a** ⊕ **b** ⊕ **C**) | 24.4% | 13.3% | 57.6% | 4.7% |
| GMCSC(**a** ⊕ **b** ⊕ **C**) | 24.5% | 11.9% | 59.2% | 4.4% |

*(b) Inverse-overlap (Gallup-Norbeck) weights*

| Wave function | 1 | 2 | 3-6 | X |
|---|---|---|---|---|
| S-BOVB (**1-6**) | 29.7% | 7.8% | 62.5% | – |
| SCGVB(**a**) | 24.5% | 10.3% | 59.8% | 5.4% |
| SCGVB(**b**) | 28.2% | 10.0% | 56.1% | 5.7% |
| SCGVB(**C**) | 23.8% | 10.2% | 61.3% | 4.8% |
| VBCI(**a** ⊕ **b** ⊕ **C**) | 24.1% | 10.2% | 61.0% | 4.7% |
| GMCSC(**a** ⊕ **b** ⊕ **C**) | 24.0% | 8.4% | 63.2% | 4.4% |

**Table S7.** **Overlap integrals and Gallup-Norbeck weights for combinations of frozen-core SCGVB wave functions for $S_2N_2$.**

| Wave function | Overlaps | | | | Weights | | |
|---|---|---|---|---|---|---|---|
| | $\langle a|b\rangle$ | $\langle a|C\rangle$ | $\langle b|C\rangle$ | $\langle C_1|C_2\rangle$ | a | b | C |
| VBCI(**a** ⊕ **b** ⊕ **C**) | 0.993 | 0.994 | 0.989 | 0.810 | 0.0% | 0.9% | 99.1% |
| GMCSC(**a** ⊕ **b** ⊕ **C**) | 0.861 | 0.911 | 0.886 | 0.744 | 19.0% | 13.6% | 67.3% |

**Table S8.  Overlaps between various frozen-core SCGVB wave functions for $S_2N_2$.**

|  | SCGVB($\mathbf{a}$) | SCGVB($\mathbf{b}$) | SCGVB($\mathbf{C}$) | VBCI($\mathbf{a} \oplus \mathbf{b} \oplus \mathbf{C}$) | GMCSC($\mathbf{a} \oplus \mathbf{b} \oplus \mathbf{C}$) |
|---|---|---|---|---|---|
| SCGVB($\mathbf{a}$) | 1 | 0.99271 | 0.99422 | 0.99467 | 0.99205 |
| SCGVB($\mathbf{b}$) | 0.99271 | 1 | 0.98897 | 0.99047 | 0.98797 |
| SCGVB($\mathbf{C}$) | 0.99422 | 0.98897 | 1 | 0.99994 | 0.99670 |
| VBCI($\mathbf{a} \oplus \mathbf{b} \oplus \mathbf{C}$) | 0.99467 | 0.99047 | 0.99994 | 1 | 0.99680 |
| GMCSC($\mathbf{a} \oplus \mathbf{b} \oplus \mathbf{C}$) | 0.99205 | 0.98797 | 0.99670 | 0.99680 | 1 |

**Table S9.  Overlaps between the normalized orthogonal complements arising from projections of various frozen-core SCGVB wave functions for $S_2N_2$.**

*(a)  BOVB*

|  | SCGVB($\mathbf{a}$) | SCGVB($\mathbf{b}$) | SCGVB($\mathbf{C}$) | VBCI($\mathbf{a} \oplus \mathbf{b} \oplus \mathbf{C}$) | GMCSC($\mathbf{a} \oplus \mathbf{b} \oplus \mathbf{C}$) |
|---|---|---|---|---|---|
| SCGVB($\mathbf{a}$) | 1 | 0.86145 | 0.88248 | 0.89080 | 0.84333 |
| SCGVB($\mathbf{b}$) | 0.86145 | 1 | 0.78478 | 0.81253 | 0.77044 |
| SCGVB($\mathbf{C}$) | 0.88248 | 0.78478 | 1 | 0.99890 | 0.93459 |
| VBCI($\mathbf{a} \oplus \mathbf{b} \oplus \mathbf{C}$) | 0.89080 | 0.81253 | 0.99890 | 1 | 0.93626 |
| GMCSC($\mathbf{a} \oplus \mathbf{b} \oplus \mathbf{C}$) | 0.84333 | 0.77044 | 0.93459 | 0.93626 | 1 |

*(b)  S-BOVB*

|  | SCGVB($\mathbf{a}$) | SCGVB($\mathbf{b}$) | SCGVB($\mathbf{C}$) | VBCI($\mathbf{a} \oplus \mathbf{b} \oplus \mathbf{C}$) | GMCSC($\mathbf{a} \oplus \mathbf{b} \oplus \mathbf{C}$) |
|---|---|---|---|---|---|
| SCGVB($\mathbf{a}$) | 1 | 0.87484 | 0.88768 | 0.89617 | 0.84577 |
| SCGVB($\mathbf{b}$) | 0.87484 | 1 | 0.80272 | 0.82952 | 0.78086 |
| SCGVB($\mathbf{C}$) | 0.88768 | 0.80272 | 1 | 0.99888 | 0.93255 |
| VBCI($\mathbf{a} \oplus \mathbf{b} \oplus \mathbf{C}$) | 0.89617 | 0.82952 | 0.99888 | 1 | 0.93395 |
| GMCSC($\mathbf{a} \oplus \mathbf{b} \oplus \mathbf{C}$) | 0.84577 | 0.78086 | 0.93255 | 0.93395 | 1 |

**Figure S2.** Symmetry-unique active orbitals in the frozen-core GMCSC($\mathbf{A} \oplus \mathbf{B}$) wave function for $S_4N_4^{2+}$. Orbitals shown in the same order as in Figure 4.
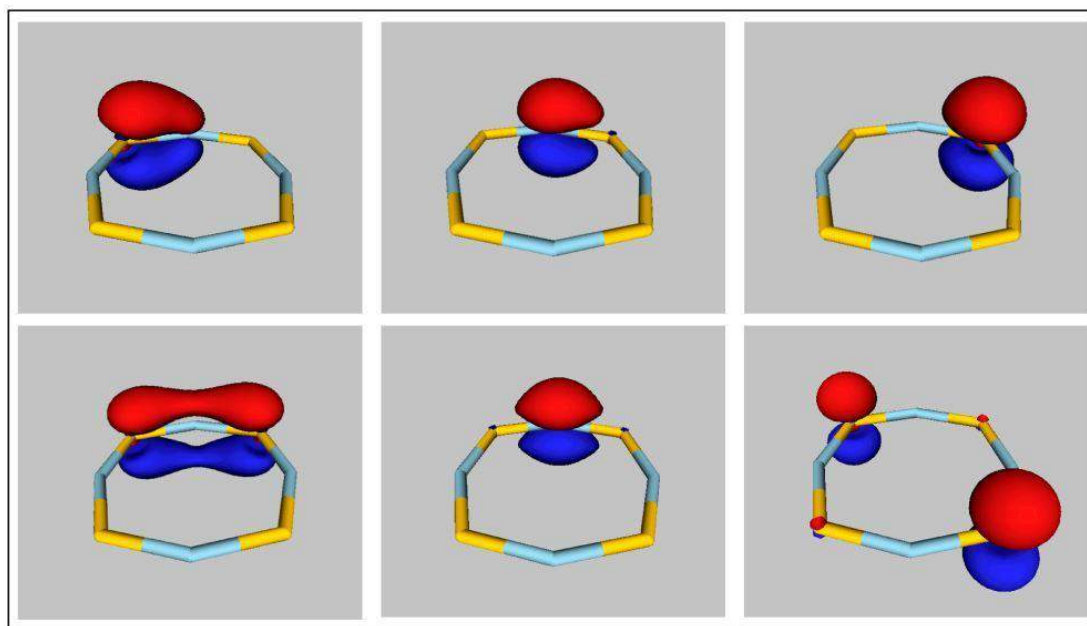


**Table S10. Component energies (in hartree) and inter-component overlaps for two-configuration wave functions.**

| System | Source of orbitals and spin-coupling coefficients | Energy of single component | Inter-component overlap |
|---|---|---|---|
| $S_2N_2$ | SCGVB($\mathbf{C}$) | -903.94607 | 0.810 |
| $S_4N_4^{2+}$ | SCGVB($\mathbf{A}$) | -1807.23764 | 0.675 |

**Table S11. Overlap integrals and Gallup-Norbeck weights for combinations of frozen-core SCGVB wave functions for $S_4N_4^{2+}$.**

| Wave function | Overlaps | | | Weights | |
|---|---|---|---|---|---|
| | $\langle \mathbf{A}|\mathbf{B}\rangle$ | $\langle \mathbf{A_1}|\mathbf{A_2}\rangle$ | $\langle \mathbf{A_1}|\mathbf{B}\rangle$ | **A** | **B** |
| VBCI($\mathbf{A} \oplus \mathbf{B}$) | 0.951 | 0.675 | 0.870 | 99.7% | 0.3% |
| GMCSC($\mathbf{A} \oplus \mathbf{B}$) | 0.847 | 0.571 | 0.751 | 86.4% | 13.6% |